

Alterations of Gut Microbiota From Colorectal Adenoma to Carcinoma

Min Jin¹, Qilin Fan^{1,2}, Linli Shi¹, Bin Zhou¹, Jingjing Wu¹, Tao Zhang¹ and Hongli Liu^{1*}

¹Cancer Center, Union Hospital, Tongji Medical College, Huazhong University of Science and Technology, Wuhan 430022, China

²Department of Gastroenterology, Central Theater General Hospital of the Chinese people's Liberation Army, Wuhan, 430070, China

*Corresponding author:

Hongli Liu,
Cancer Center, Union Hospital, Tongji Medical
College, Huazhong University of Science and
Technology, Wuhan 430022, China,
E-mail: hongli_liu@hust.edu.cn

Received: 14 Apr 2022

Accepted: 02 May 2022

Published: 06 May 2022

J Short Name: COO

Copyright:

©2022 Hongli Liu. This is an open access article distributed under the terms of the Creative Commons Attribution License, which permits unrestricted use, distribution, and build upon your work non-commercially.

Keywords:

Gut microbiota; 16S rRNA gene sequencing;
Colorectal cancer; Colorectal adenoma;
Fusobacteria

Citation:

Hongli Liu, Alterations of Gut Microbiota From Colorectal Adenoma to Carcinoma. Clin Onco. 2022; 6(5): 1-11

1. Abstract

Gut microbiota has been implicated as a critical role in the development of colorectal cancer (CRC) and colorectal adenoma (CRA). However, few basic research has revealed the association between gut microbiota and the development of CRA and CRC. We aim to compare the diversity and composition of intestinal flora in CRA and CRC patients, to reveal the changes of intestinal microorganism in the evolution of normal intestinal mucosa-CRA-CRC axis, and to explore potential biomarkers. We analysed colorectal tissues (11 CRC, 11 CRA and 11 healthy volunteers (HC)). Using 16S rRNA sequencing analysis to compare the gut microbiome of patients with CRC, CRA and HC. The microbial diversity including alpha diversity, beta diversity and identified the microbial compositions among the three groups were characterized. Intestinal microbial composition and diversity were significantly decreased in the CRA group, whereas those were obviously increased in the CRC group. The fourth most predominant microbial compositions in the three groups were *Proteobacteria*, *Firmicutes*, *Actinobacteria* and *Bacteroidetes* at the phylum level. Moreover, the relative abundance of *Fusobacteria* at the phylum level behaved a general trend of decreasing in CRA group first and then increasing in CRC group. When exploring the *Fusobacteria* abundance in MetaCyc database signaling in different groups, it was indicated that *Fusobacteria* was also higher in CRC than CRA especially in the ICME2-PWY, Cobalsyn-PWY and Anaglycolysi signal pathways. Taken together, the observed intestinal microbial difference among the three groups provides a basis for understanding the potential role of intestinal microorganism in the evolution

of normal intestinal mucosa-CRA-CRC axis.

2. Introduction

Colorectal cancer (CRC) is one of most common malignancies and the second leading cause of death among malignant tumors worldwide [1,2]. It mainly stems from an adenomatous polyp then grows into advanced colorectal adenoma (CRA) with highgrade dysplasia, and finally evolves intoaggressive cancer [3]. Many explicit environmental factors, such as unhealthy diet and lifestyle, are vital for the intestinal microbiome composition and function, which can generate the individual gene expression, physiological metabolic regulation, and immune response, thereby influencing cancer development [4]. Based on previous studies, intestinal microbiota has been considered to play a key role in colorectal tumorigenesis, which may ulteriorly promote CRC development through microbial metabolites, inflammatory pathways or the interference in the energy balance of cancer cells [5,6]. Yang Y et al indicated a potential intimate relationship between gut microbiome and biometabolome in CRC [7]. Metabolites promote genotoxicity and inhibit or promote tumors through a variety of mechanisms, such as altered metabolic pathways to promote anabolism, competitive enzyme inhibition, and signaling protein modification [8,9]. De Martel C et al found that intestinal flora might be an important etiological factor for liver cancer, gastric cancer and intestinal tumor [10-14]. Another study has shown that microbial composition has potential significance for the early detection and prevention of esophageal cancer [15]. Microbiome dysregulation is a change in the composition of bacteria [16]. The study of microbiota dysregulation is of great significance for exploring the carcinogenic

mechanism of CRC [17-20]. For example, *Fusobacterium nucleatum* is prevalent in CRC and precancerous lesions with poor prognosis [21-23]. However, few studies have studied and clarified the characteristics and differences in the involvement of normal intestinal mucosa-CRA-CRC axial pathway model [24,25]. In our study, we will reveal the potential characteristics and differences of intestinal microbial composition during its evolution along the above-mentioned axes, and further explore novel biomarkers for CRA and CRC.

3. Material and Methods

3.1. General Information About Patients Enrolled

A total of 11 CRA subjects from our hospital were followed up regularly January 30,2015 to December 30,2018. There were 6 males and 5 females in CRA. There were 8 cases of rectum, 1 case of sigmoid colon, and 2 cases of colon. The maximum tumor diameter was 4 cm or greater in 8 cases, and less than 4 cm in 3 cases. All of these cases were isolated. Besides that a total of 11 CRA subjects and 11 healthy volunteers tissue were included from Department of Gastroenterology, Wuhan Eighth Hospital from January 2015 to December 2018. There were 5 males and 6 females in colorectal adenomas. There were 8 cases of rectum, 2 cases of sigmoid colon, and 1 case of colon. The last follow-up time was August 30, 2019.

3.2. Inclusion and Exclusion Criteria

Inclusion criteria: 1) Age range from 20 to 70 years old; 2) The pathological diagnosis of CRA group and CRC group was colorectal adenoma and colorectal adenocarcinoma, respectively; 3) No previous surgery, chemoradiotherapy or targeted immunotherapy. Exclusion criteria: 1) Previous history of colorectal surgery, familial adenomatous polyposis or hereditary non-polyposis colorectal cancer, inflammatory bowel disease, metabolic diseases, infectious diseases, liver and kidney diseases, and immunodeficiency diseases; 2) Use of antibiotics or corticosteroids or probiotics; 3) Have

special eating habits; 4) Body mass index is outside the normal range.

3.3. Sample Collection, DNA Extraction and PCR Amplification

Two tissue specimens were collected from the included population, one of which was routinely stored in formalin and sent to the Department of Pathology, and the other specimen was immediately labeled and placed in a -80°C refrigerator for analysis. We extracted DNA from the collected samples, used Illumina sequencing [26] method and PCR to amplify the V3-V4 variable region of 16S rRNA of bacterial genome. 5'-ACTCCTACGGGAGGCAGCA-3' and 5'-GGACTACHVGGGTWCTAAT-3' were the upper and lower primer sequences respectively.

3.4. Bioinformatics and Statistical Analysis

QIIME 2.0 [27,28] were used to analyze the obtained sequences. According to the total number of ASV/OTUs corresponding to each sample in the ASV/OTUs abundance matrix, software R was used to draw rarefaction curve, species accumulation curves and rank abundance curve respectively. We used PICRUSt2.0 from KEGG database and MetaCyc database to predict the microbial metabolism functions. The statistical methods used mainly included chi-squared test and t-test.

4. Results

4.1. Participant Information and Study Design

A total of 33 tissue samples were analyzed in this study, including 11 from HC, 11 from CRA and 11 from CRC (Figure 1). There were 16 samples were male and 17 were female. There were no significant differences in age, gender, tumor localization, smoking status and underlying disease among the three groups. And there were significant statistical differences in surgery status ($p<0.001$) and antibiotic usage ($p<0.05$). Detailed clinical data of the subjects are shown in Table 1.

Table 1: Clinical characteristics of the enrolled participants.

Characteristics	Patients (n=33)			p
	HC(n=11)	CRA(n=11)	CRC(n=11)	
Age, year				
Mean ± SD	66.55±8.45	66.55±8.45	61.64±8.12	0.45
Sex				
Female	6(54.50%)	6(54.50%)	5(45.50%)	0.89
Male	5(45.50%)	5(45.50%)	6(54.50%)	
Tumor Localization				
colon	3(27.28%)	1(9.09%)	2(18.18%)	0.33
Sigmoid	4(36.36%)	2(18.18%)	1(9.09%)	
Rectum	4(36.36%)	8(72.73%)	8(72.73%)	
TNM Stage				
Stage I			5(45.50%)	
Stage II			3(27.28%)	
Stage III			2(18.18%)	
Stage IV			1 (9.04%)	

Smoking status				
Smoker	3(27.27%)	3(27.27%)	2(18.18%)	0.33
No smoker	8(72.73%)	8(72.73%)	9(81.82%)	
Underlying disease				
Hypertension	1(9.09%)	4(36.36%)	1(9.09%)	
Hypercholesterolemia	2(18.18%)	3(27.28%)	2(18.18%)	
Diabetes	8(72.73%)	4(36.36%)	8(72.73%)	

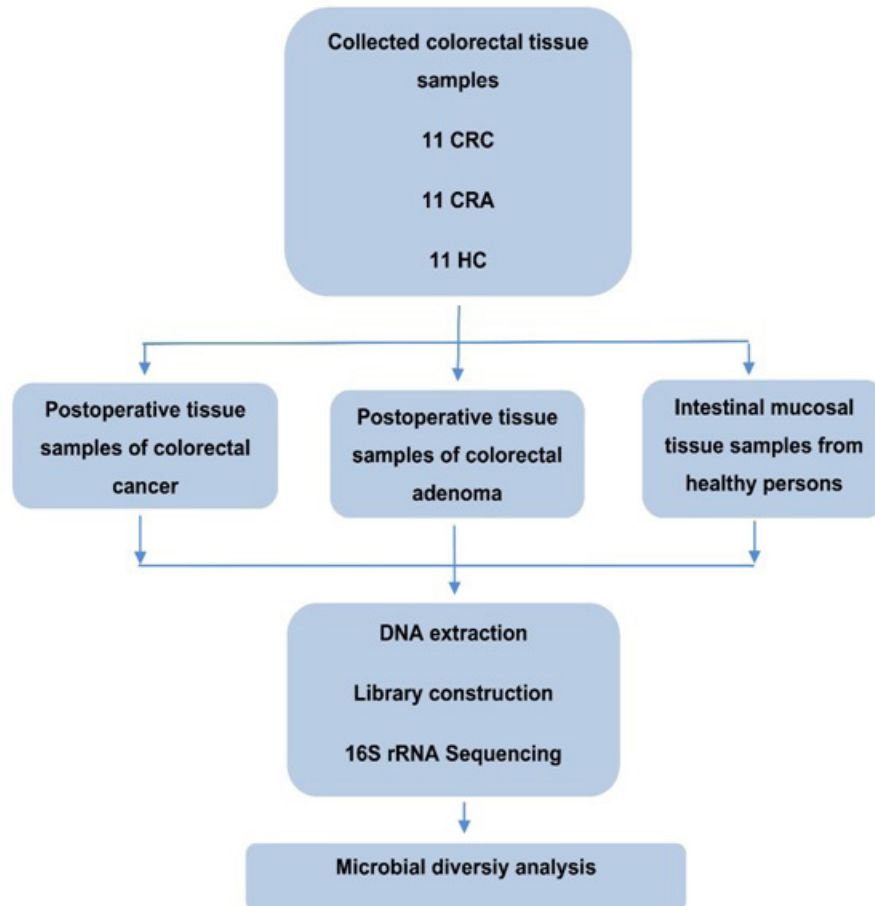


Figure 1: Study design and flow diagram. Consecutive gut tissue samples were prospectively collected from 11 healthy controls, 11 patients with CRA, and 11 patients with CRC according to the inclusion criteria. Then we characterized the gut microbiome among 3 groups, identified microbial markers.

4.2. Estimation of Sequencing Depth

On sequencing 16SrDNA of 33 samples, a total of 1188302 usable high quality sequences were obtained in three groups. According to the correspondence between the sequence similarity and bacterial taxonomic status, 97% similarity is generally considered to species division. The rarefaction curves indicated that the sequencing depth was sufficient (Figure 2A). The species accumulation curves indicated that the sequencing volume of each sample had reached saturation (Figure 2B). Abundance grade curves were used to assess the relative homogeneity of bacteria, and all samples showed a similar pattern (Figure 2C). Furthermore, a Venn diagram displaying the overlaps among three groups was shown in Figure 2D.

4.3. Diversity of Intestinal Microbiota

We analyzed and evaluated the differences in richness, diversity and evenness among the three groups of bacteria with alpha-diversity index. The results indicated that the gut microbial diversity was significantly lower in the CRA group than the HC group according to the CHAO1 index and Observed_species ($p < 0.05$), but was obviously higher in CRC group than the HC group according to the Shannon and Observed_species ($p < 0.05$), and dramatically richer in the CRC group than the CRA group according to the CHAO1, Faith_d, Observed_species index ($p < 0.001$) and Shannon index ($p < 0.05$) (Figure 3A). Moreover, we compared the similarity and difference degree of communities among three groups of samples with beta-diversity analysis (Figure 3B-C). The results were similar to the alpha-diversity analysis. Significant clustering

was observed among the HC, CRA, and CRC groups. A significant clustering was formed as the CRC group was distinguished from the CRA and the HC group, while the CRA group and HC group

has partial overlapping. In summary, the results suggested that gut microbial diversity was reduced in the CRA group, but increased significantly in the CRC group.

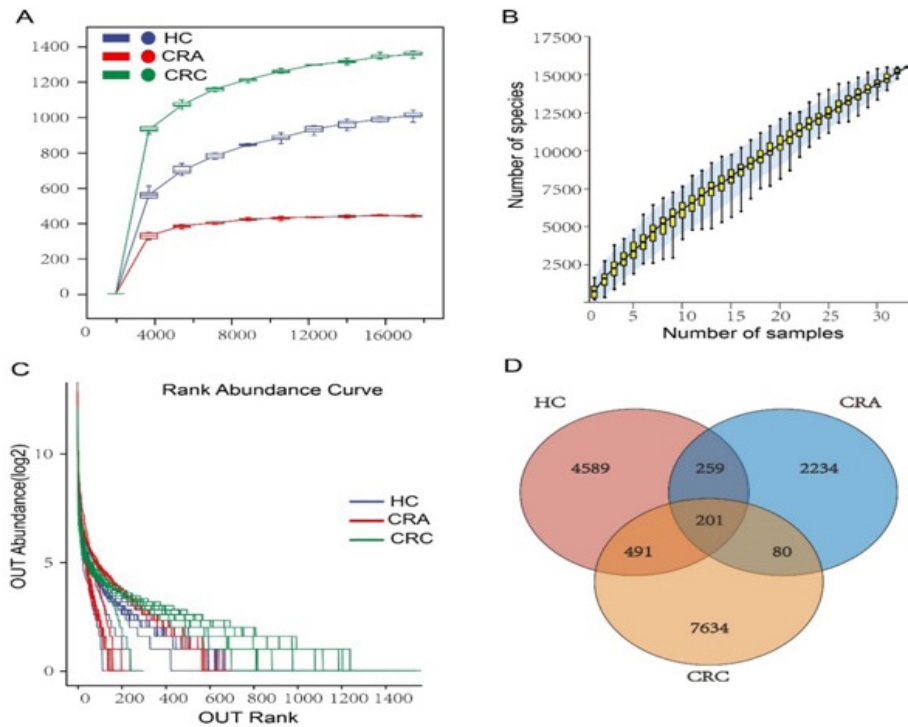


Figure 2. Estimation of sample depth and Venn diagram in the HC, CRA, and CRC groups. (A) The dilution curve. (B) Species accumulation curve between number of samples. (C) The relative bacterial evenness was evaluated by the rank abundance curves. (D) Venn diagram at species level. HC, healthy volunteers; CRA, colorectal cancer; CRC, colorectal adenoma. OTU, operational taxonomy unit.

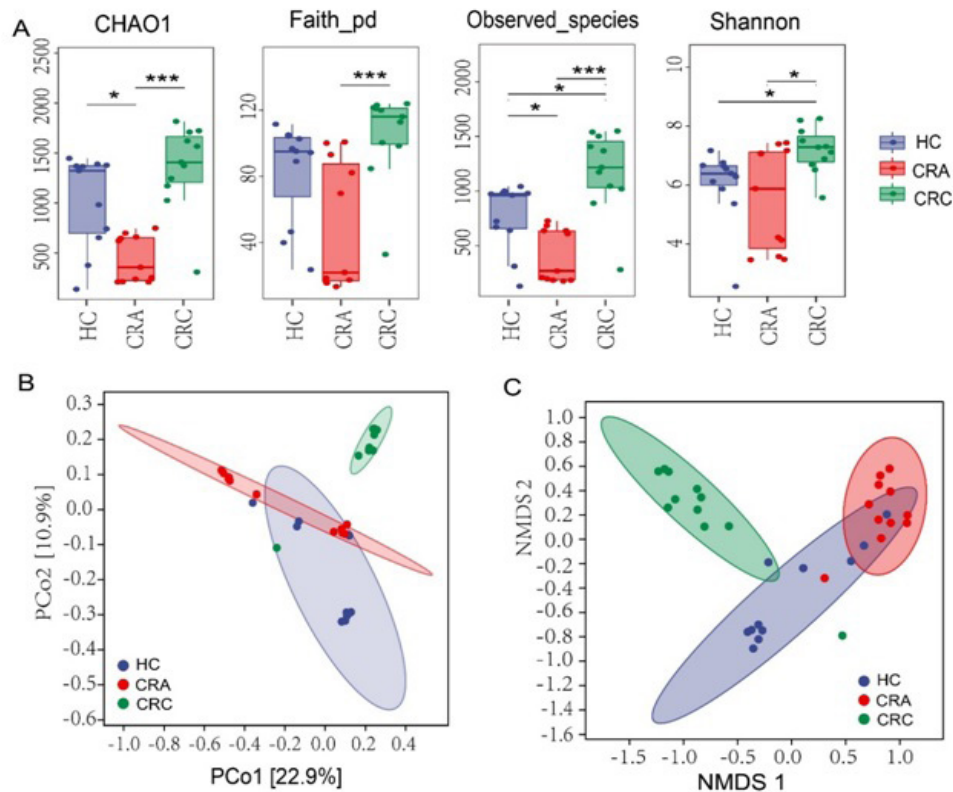


Figure 3. Microbial community richness and Alpha diversity among the HC, CRA, and CRC groups. (A) Gut microbial diversity was estimated by the Chao1, Faith_pd, Observed_species and Shannon index. (B) PCoA analysis based on unweighted UniFrac distance matrix. (C) Beta diversity was calculated using unweighted UniFrac by NMDS. Data are shown as the mean \pm SD, * $P < 0.05$, ** $P < 0.01$, *** $P < 0.001$. HC, healthy volunteers; CRA, colorectal cancer; CRC, colorectal adenoma. PCoA, principal coordinates analysis; NMDS, nonmetric multidimensional scaling.

4.4. Microbiota Composition at The Phylum Levels

Meanwhile, we examined the microbiota composition differences at the phylum in HC, CRA and CRC groups. Proteobacteria was the most abundant phyla, accounting for 75.6% of the total intestinal flora. Firmicutes, Actinobacteria and Bacteroidetes accounted for 7.75%, 4.8% and 4.28% of the total intestinal flora, respectively (Supplementary Table 1). After statistical analysis based on the mean value within the group, it was indicated that Fusobacteria was reduced in the CRA (0.04%) group, but increased in the CRC group (0.254%) (Figure 4A-B, Supplementary Table 2). The species composition heat map also consistently showed that Fusobac-

teria in the CRC group (2.79%) was significantly richer than that in the CRA group (0.41%) (Figure 4C, Supplementary Table 3) at the phylum level. LEfSe analysis with an LDA score ≥ 4.0 was also conducted among the HC, CRA and CRC groups. As shown in Figure 5, the microflora of the CRC patients was enriched with *c_Alphaproteobacteria*, *f_Sphingomonadaceae*, *p_Acidobacteria* and *g_Kaistobacter*. However, increased abundances of *c_Gammaproteobacteria*, *o_Pseudomonadales*, *g_Acinetobacter*, *f_Moraxellaceae*, *o_Lactobacillales*, *g_Xanthomonadales*, *f_Streptococcaceae*, *g_Streptococcus* and *f_Pseudomonadaceae* were observed in the CRA group.

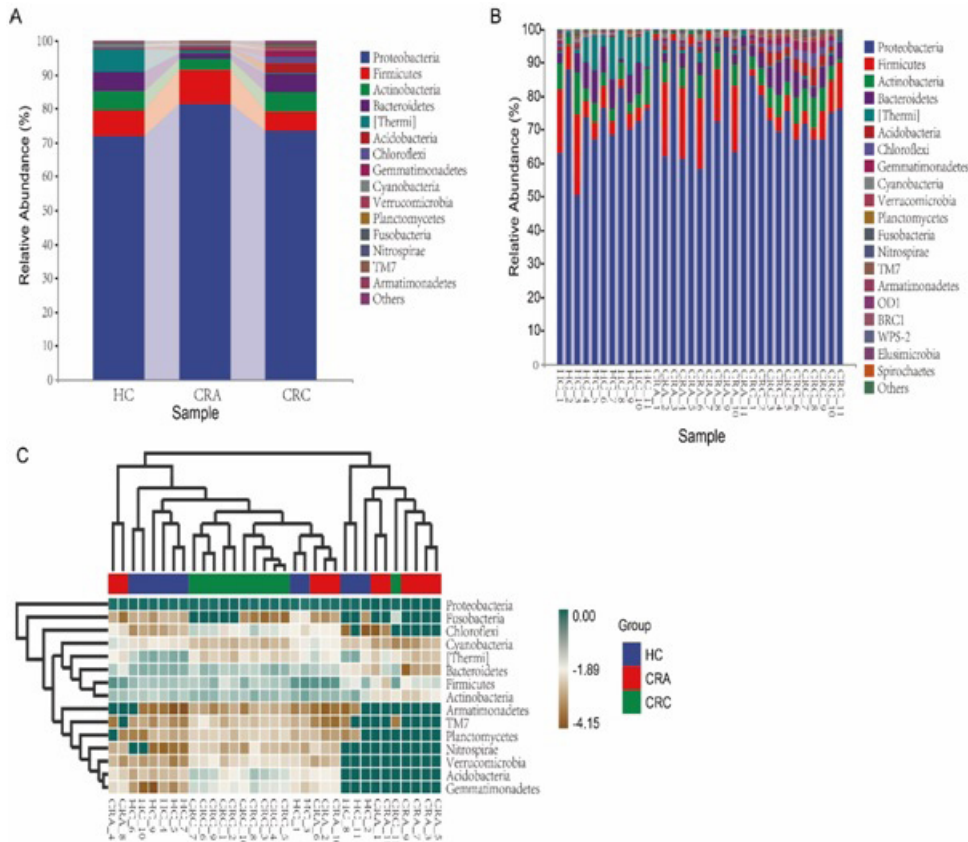


Figure 4: Gut microbiota composition at the phylum levels. (A-B) Average composition of bacterial community at the phylum levels. (C) The species composition heat map.

Supplementary Table 1: Microbial taxa at the phylum levels within the three groups of HC, CRA and CRC.

Microbiota ID	Overall
Proteobacteria	0.755593
Firmicutes	0.077482
Actinobacteria	0.048021
Bacteroidetes	0.042808
[Thermi]	0.027291
Acidobacteria	0.01124
Chloroflexi	0.00918
Gemmatimonadetes	0.007735
Cyanobacteria	0.006139
Verrucomicrobia	0.002859
Planctomycetes	0.001936
Fusobacteria	0.001808
Nitrospirae	0.001584
TM7	0.001551
Armatimonadetes	0.000454
Others	0.004317
	1

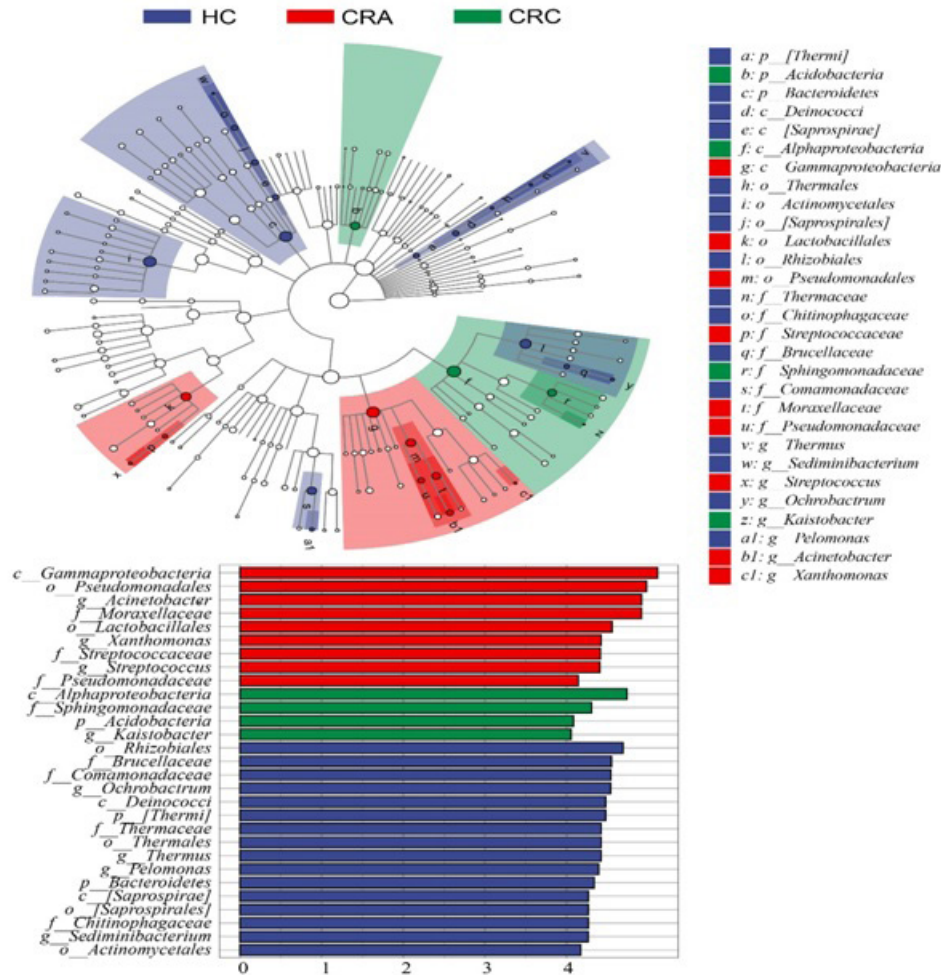


Figure 5: LefSe analysis among the HC, CRA, and CRC groups. The differentially abundant taxa in the taxonomic tree are shown in the cladogram in different colors. The LDA scores greater than 4.0 for the significantly differentially abundant bacteria are displayed in the histogram with different colors. HC, healthy volunteers; CRA, colorectal cancer; CRC, colorectal adenoma; LefSe, linear discriminant effect size; LDA, linear discriminant analysis

Supplementary Table 2: The mean value of taxonomic composition of the microbiota among the group of HC, CRA and CRC at the phylum levels.

ID	HC	CRA	CRC
Proteobacteria	0.717721	0.813776	0.735283
Firmicutes	0.076174	0.100186	0.056086
Actinobacteria	0.056610	0.031743	0.055711
Bacteroidetes	0.057473	0.017146	0.053804
[Thermi]	0.066566	0.009677	0.005631
Acidobacteria	0.002972	0.004228	0.026520
Chloroflexi	0.002419	0.004967	0.020155
Gemmatimonadetes	0.001381	0.003664	0.018160
Cyanobacteria	0.007664	0.008621	0.002131
Verrucomicrobia	0.001408	0.000807	0.006362
Planctomycetes	0.001207	0.000437	0.004163
Fusobacteria	0.001516	0.000371	0.002536
Nitrospirae	0.000385	0.001295	0.003073
TM7	0.000865	0.000100	0.003689
Armatimonadetes	0.000213	0.000048	0.001101
OD1	0.000599	0.000192	0.000467
BRC1	0	0	0.000913

WPS-2	0.000592	0.000067	0.000229
Elusimicrobia	0.000219	0.000062	0.000410
Spirochaetes	0.000246	0.000034	0.000136
Chlorobi	0.000049	0.000062	0.000234
Tenericutes	0.000102	0.000056	0.000170
AD3	0.000179	0.000012	0.000137
Deferribacteres	0.000031	0.000167	0.000051
WS3	0.000065	0.000062	0.000114
Others	0.002343	0.002219	0.002733

Supplementary Table 3: Relative abundances of bacterial taxa per sample corresponding to species Composition Heat map at the phylum levels.

sample	Proteo bacteria	Firmi cutes	Actino bacteria	Bacter oidetes	[Thermi]	Acido bacteria	Chloroflexi	Gemmat imonadetes	Cyano bacteria	Verru comicrobia	Plancto mycetes	Fuso bacteria	Nitro spirae	TM7	Armati monadetes
HC_1	0.6315	0.1897	0.0777	0.0291	0.0063	0.0100	0.0129	0.0078	0.0091	0.0063	0.0015	0.0083	0.0025	0.0017	0.0003
HC_2	0.8799	0.0739	0.0254	0.0045	0.0097	0.0000	0.0001	0.0000	0.0055	0.0000	0.0000	0.0007	0.0000	0.0000	0.0000
HC_3	0.5061	0.2402	0.1246	0.0582	0.0143	0.0077	0.0056	0.0032	0.0143	0.0035	0.0029	0.0094	0.0010	0.0023	0.0006
HC_4	0.7375	0.0494	0.0367	0.0791	0.0693	0.0023	0.0010	0.0013	0.0099	0.0015	0.0022	0.0022	0.0001	0.0016	0.0002
HC_5	0.6717	0.0498	0.0576	0.0978	0.1020	0.0024	0.0019	0.0004	0.0076	0.0003	0.0011	0.0021	0.0002	0.0005	0.0001
HC_6	0.7671	0.0649	0.0378	0.0781	0.0322	0.0012	0.0005	0.0008	0.0075	0.0015	0.0004	0.0015	0.0000	0.0009	0.0000
HC_7	0.6857	0.0411	0.0371	0.0882	0.1230	0.0043	0.0025	0.0015	0.0078	0.0005	0.0013	0.0013	0.0002	0.0003	0.0001
HC_8	0.8273	0.0220	0.0536	0.0094	0.0830	0.0000	0.0002	0.0000	0.0032	0.0000	0.0004	0.0000	0.0000	0.0004	0.0001
HC_9	0.7005	0.0496	0.0290	0.0861	0.1085	0.0016	0.0008	0.0001	0.0104	0.0011	0.0021	0.0006	0.0002	0.0005	0.0002
HC_10	0.7255	0.0419	0.0398	0.0938	0.0792	0.0033	0.0012	0.0001	0.0058	0.0007	0.0003	0.0015	0.0000	0.0014	0.0002
HC_11	0.7621	0.0154	0.1034	0.0079	0.1047	0.0000	0.0000	0.0000	0.0032	0.0000	0.0010	0.0000	0.0000	0.0000	0.0005
CRA_1	0.9695	0.0169	0.0070	0.0019	0.0038	0.0000	0.0001	0.0000	0.0009	0.0000	0.0000	0.0000	0.0000	0.0000	0.0000
CRA_2	0.6191	0.2201	0.0629	0.0271	0.0093	0.0124	0.0130	0.0104	0.0127	0.0018	0.0008	0.0005	0.0027	0.0002	0.0001
CRA_3	0.9647	0.0216	0.0080	0.0012	0.0027	0.0000	0.0000	0.0000	0.0018	0.0000	0.0000	0.0000	0.0000	0.0000	0.0000
CRA_4	0.6137	0.2142	0.0584	0.0409	0.0127	0.0079	0.0113	0.0060	0.0226	0.0022	0.0000	0.0015	0.0015	0.0003	0.0000
CRA_5	0.9539	0.0276	0.0114	0.0012	0.0033	0.0000	0.0000	0.0000	0.0025	0.0000	0.0000	0.0000	0.0000	0.0000	0.0000
CRA_6	0.5813	0.2111	0.0706	0.0397	0.0302	0.0114	0.0117	0.0064	0.0203	0.0011	0.0026	0.0006	0.0058	0.0004	0.0002
CRA_7	0.9704	0.0223	0.0036	0.0010	0.0019	0.0000	0.0000	0.0000	0.0007	0.0000	0.0000	0.0000	0.0000	0.0000	0.0000
CRA_8	0.7249	0.1563	0.0515	0.0171	0.0068	0.0041	0.0061	0.0077	0.0179	0.0006	0.0004	0.0002	0.0020	0.0000	0.0000
CRA_9	0.9803	0.0116	0.0036	0.0001	0.0038	0.0000	0.0000	0.0000	0.0005	0.0000	0.0000	0.0000	0.0000	0.0000	0.0000
CRA_10	0.6322	0.1975	0.0664	0.0296	0.0128	0.0107	0.0120	0.0099	0.0135	0.0032	0.0010	0.0013	0.0022	0.0002	0.0002
CRA_11	0.9416	0.0029	0.0058	0.0288	0.0190	0.0000	0.0004	0.0000	0.0014	0.0000	0.0000	0.0000	0.0000	0.0000	0.0000
CRC_T1	0.8604	0.0196	0.0377	0.0351	0.0041	0.0081	0.0068	0.0122	0.0023	0.0023	0.0048	0.0000	0.0010	0.0013	0.0007
CRC_T2	0.8016	0.0319	0.0527	0.0446	0.0019	0.0130	0.0146	0.0172	0.0016	0.0054	0.0021	0.0003	0.0018	0.0029	0.0016
CRC_T3	0.7284	0.0364	0.0608	0.0585	0.0086	0.0389	0.0195	0.0196	0.0015	0.0068	0.0060	0.0002	0.0025	0.0038	0.0022
CRC_T4	0.6940	0.0457	0.0622	0.0991	0.0039	0.0283	0.0207	0.0182	0.0023	0.0083	0.0037	0.0003	0.0025	0.0042	0.0013
CRC_T5	0.7566	0.0463	0.0402	0.0735	0.0045	0.0232	0.0142	0.0168	0.0020	0.0065	0.0060	0.0002	0.0017	0.0032	0.0016
CRC_T6	0.6715	0.0477	0.0773	0.0771	0.0026	0.0364	0.0272	0.0265	0.0022	0.0072	0.0042	0.0005	0.0040	0.0105	0.0011
CRC_T7	0.7196	0.0368	0.0684	0.0260	0.0092	0.0427	0.0334	0.0261	0.0028	0.0065	0.0050	0.0004	0.0060	0.0048	0.0014
CRC_T8	0.6698	0.0345	0.0911	0.0316	0.0044	0.0538	0.0435	0.0330	0.0027	0.0100	0.0047	0.0003	0.0098	0.0024	0.0016
CRC_T9	0.6700	0.0855	0.0699	0.0613	0.0049	0.0286	0.0261	0.0181	0.0028	0.0117	0.0049	0.0001	0.0040	0.0037	0.0004
CRC_T10	0.7519	0.0950	0.0431	0.0331	0.0090	0.0187	0.0157	0.0121	0.0029	0.0053	0.0045	0.0006	0.0006	0.0034	0.0003
CRC_T11	0.7643	0.1375	0.0093	0.0520	0.0087	0.0000	0.0000	0.0000	0.0004	0.0000	0.0000	0.0265	0.0000	0.0003	0.0000

Supplementary Table 4: Statistically significant signaling pathways enriched in pairwise comparisons between groups.

CRA & CRC					
pathway	description	logFC	SE	Pvalues	adjPvalues
PWY-5743	3-hydroxypropanoate cycle	1.8550000	0.3193000	0.00000001	0.0000027
PWY-5744	glyoxylate assimilation	1.6720000	0.3171000	0.0000001	0.0000290
PWY-7024	superpathway of the 3-hydroxypropanoate cycle	1.6190000	0.3160000	0.0000003	0.0000438
DENITRIFICATION-PWY	nitrate reduction I (denitrification)	-1.2890000	0.3761000	0.0006102	0.0330300
PWY-7031	protein N-glycosylation (bacterial)	-1.9040000	0.5353000	0.0003740	0.0231300
PWY-7046	4-coumarate degradation (anaerobic)	-2.9050000	0.7515000	0.0001110	0.0080100
PWY-6174	mevalonate pathway II (archaea)	-4.0580000	0.8570000	0.0000022	0.0001897
PWY-7391	isoprene biosynthesis II (engineered)	-4.2470000	0.8852000	0.0000016	0.0001740
HC & CRC					
PWY-3801	sucrose degradation II (sucrose synthase)	-2.1770000	0.5645000	0.0001149	0.0256800
PWY-5392	reductive TCA cycle II	-2.9640000	0.5894000	0.0000005	0.0002198
HC & CRA					
PWY-1882	superpathway of C1 compounds oxidation to CO2	1.7260000	0.4691000	0.0002338	0.0847400
PWY-7391	isoprene biosynthesis II (engineered)	2.8540000	0.8031000	0.0003792	0.0847400

4.5. Prediction Analysis of Functional Potential of Intestinal Microbiota

The imbalance of microflora can cause metabolic changes in the system [26,27], while metabolic disorders can in turn affect the composition of microflora [28]. PICRUSt2 refer to KEGG and MetaCyc database to study the Phylogenetic characteristics of all OUT [29]. Picrust2 analysis showed that there were 12 KEGG pathways with significant abundance differences between CRA and CRC groups (Supplementary Figure 1A). There were also 12 significant abundance differences between the CRC group and the HC group (Supplementary Figure 1B). And there were 11 KEGG pathways with significant abundance differences between the CRA group and the HC group (Supplementary Figure 1C). Further results showed that the relative abundances of 2 sugurose metabolism-related pathways (PWY-5392, $p < 0.001$; PWY-3801, $p < 0.01$) was significantly increased in the CRC group than in the HC group (Figure 5). The relative abundances of 5 Degradation/Utilization-related pathways (PWY-6486, P21-PWY, $p < 0.001$; PWY-7046, PWY-1361, $p < 0.01$; P164-PWY, $p < 0.05$), 5 Biosynthesis -related pathways (PWY-7391, PWY-6174, PWY-1882, $p < 0.001$; PWY-7031, DENITRIFICATION-PWY, $p < 0.05$) were significantly higher in the CRC group than in the CRA group,

while the abundances of 3 C1 compound utilization-related pathways were significantly lower in the CRC group than in the CRA group (PWY-7024, PWY-5744, PWY-5743, $p < 0.001$) (Figure 5). However, there was no significantly different pathways between CRA group and HC group. Therefore, these results suggest that metabolic significantly changes in CRC individuals.

Previously, it was described that Fusobacteria was expressed in high levels in CRC while the Fusobacteria expression was linked to clinical and pathological parameters. After analysis of the microbiota composition among the three group, we consistently found that the abundance of Fusobacteria was higher in CRC and CRA group than HC group (Figure 4C). As a target of interest, we further explored the abundance of Fusobacteria in different KEGG signaling pathways in the different groups. We interestingly found that in 2 pathways of Cofactor, Prosthetic Group, Electron Carrier and Vitamin Biosynthesis (ICME2-PWY and Anaglycolysis-PWY), 1 pathways of Glycolysis (ANAGLYCOLYSIS-PWY) and 1 pathways of Short-Chain Fatty Acids Fermentation (AN-AEROFRUCAT-PWY), expression of Fusobacteria in HC tissues, CRA tissues, and CRC tissues is descending in turn (Figure 6 and Figure 7).

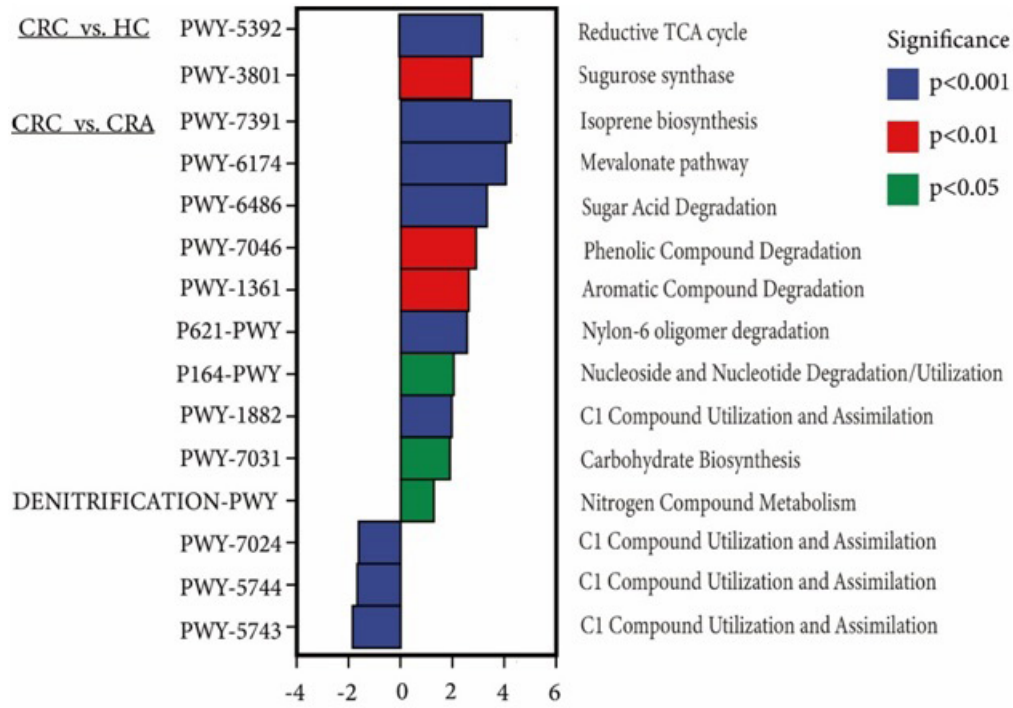


Figure 6. Metabolic pathway analysis with p-value ≤ 0.05. In the horizontal axis, positive values of LOGFC (LOG2 (fold change)) represent up-regulation in the upregulated group compared with the control group, and negative values represent down-regulation. The vertical coordinates are different Pathway/Group tags, which indicated the degree of significance in different colors.

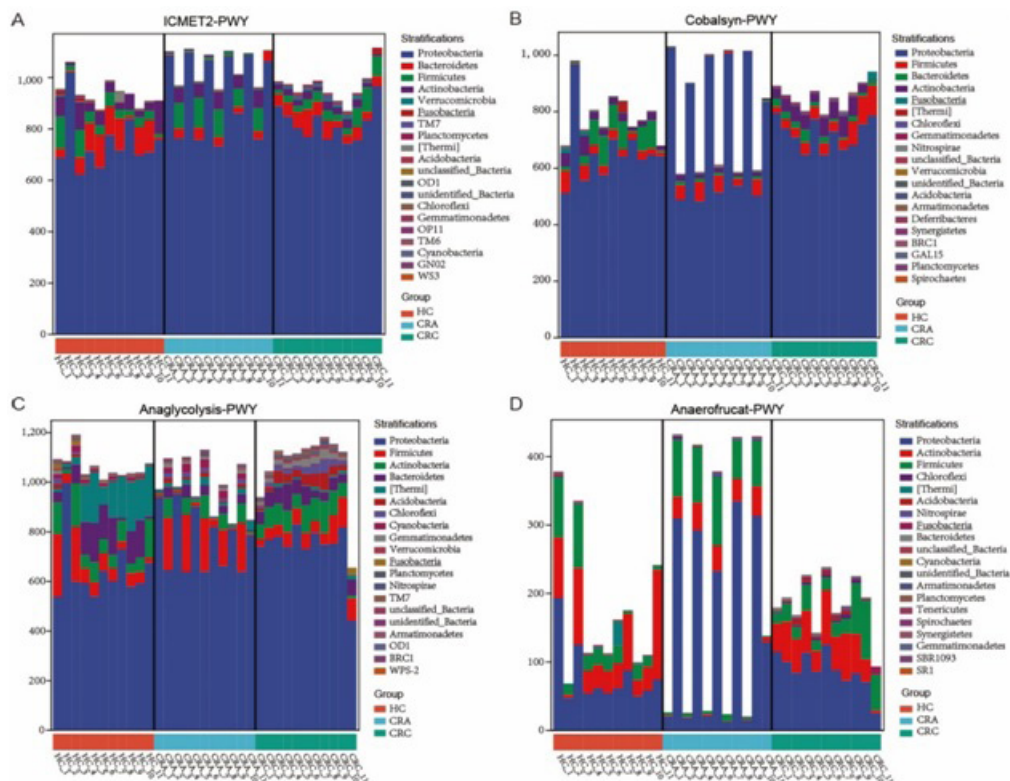


Figure 7: Species composition in four different metabolic pathways at the genus level. The contribution ratio of different taxa to this metabolic pathway in ICME2-PWY (A), Cobalsyn-PWY (B), Anaglycolysi (C) and Anaerofrucat (D) signal pathway was shown by different color stratification. The abscissa is the sample label; the ordinate is the relative abundance of related metabolic pathways.

5. Discussion

The potentially important role of gut microbiota in the initiation and progression of CRC has been extensively studied, especially in CRC, but the potential impact and dynamic change of gut microbiota on CRA-CRC is far from clear. Studies on the component and characteristics of intestinal microbiota between CRA and CRC patients and healthy people mostly use samples such as feces, oral or pharyngeal swabs of subjects, and studies using intestinal tissue samples are rare. To the best of our knowledge, this study is the earliest to use CRA, CRC and HC tissue samples in South China to reveal the characteristics of intestinal microbiome community structure, microbial diversity and predict the potential function based on intestinal microbiota ASV/ OTUs. First, we assessed the diversity of the intestinal microbiome in the three groups and found that the tissue microbial diversity was memorably decreased in the CRA group when compared with the HC group but observably increased from CRA to CRC. Previous studies have shown that *Fusobacteria* is associated with CRC [21,30,31], and *Fusobacteria* may be the "driving factor" of CRC [32]. In addition, numerous studies have indicated that *Fusobacterium nucleatum* is more enriched in CRC tumor tissues than CRA [32,22]. Our results consistently indicated that *Fusobacteria* expressed higher enrichment in CRC than CRA, but the curve of the expression trend of *Fusobacteria* looked like a "V" (It fell first in CRA, and then rose in CRC). This research interestingly suggests that *Fusobacterium* may play diverse roles at different stages of normal intestinal mucosa-CRA-CRC axis, but the mechanism between the different abundance of *Fusobacterium* in intestinal tissues requires further investigation. We then demonstrated that the development of CRC is accompanied by changes in intestinal flora. It is generally believed that the development of most CRC is a continuous process, usually following the normal mucosa-CRA-CRC sequence axis model [34]. Our results suggest that the gut microbiome also exhibits dynamic changes as CRC progresses. The main microflora of the three groups were Proteobacteria, Firmicutes, Actinobacteria and Bacteroidetes at the phylum level. This is consistent with previous research. Feng et al. [14] also confirmed the development and change of intestinal flora along the colorectal adenoma-carcinoma sequence axis through shotgun sequencing of fecal samples, and similar results were obtained by Nakatsu [35]. Finally, we used PICRUSt2 to analyze the potential function of intestinal flora. The research findings showed that the metabolic of xenobiotics by cytochrome P450 signaling pathway was increased in the CRC group and the mannosylglycerate biosynthesis I signaling pathway was increased in the CRA group compared with HC group. Compared with CRC group, Endocytosis signal pathway was significantly increased in the CRA group. Meera et al [36] et al showed that the expression of Metabolism of xenobiotics by cytochrome P450 was increased in colorectal cancer by microarray analysis, and also showed that high expression of P450-CYP51/CYP2S1

was associated with poor prognosis in colorectal cancer. Letizia Lanzetti et al [37] showed that endocytosis plays a key role in the occurrence and development of human diseases, especially cancer, and is a potential carcinogenic pathway. This is consistent with the conclusion of significant increase of Endocytosis signal pathway in the CRA group in our study. This study includes a number of notable advantages and limitations. As is known to all, tissue samples are conducive to identify the microbiome during the initiation and development of CRC. In addition to this, we have analyzed clinical variables as thoroughly as possible. However, there are some defects to the research. First of all, our research only compared the diversity in the component and structural characteristics of intestinal microflora among the three groups, and simply predicted the potential function of intestinal microflora through PICRUSt2, but did not study the potential mechanism of colorectal tumors. Secondly, we only conducted a single center study, rather than a multi-center study, and included a small sample size, while the component and activity of the intestinal flora lies on many factors. These biomarkers of intestinal flora are significantly ethnically dependent and should be validated in a wide range of populations, so the existing data sets may be untypical and unrepresentative. Thirdly, there are various sampling methods for the study of intestinal flora, such as intestinal tissue, fecal sample and oral sample. In this study, only intestinal tissue samples were used, which may lead to bias of the results.

6. Conclusion

In conclusion, we prove that the microbiome characteristics in CRC, CRA and HC tissue samples, explored the underlying characteristics and differences of intestinal microbial composition in the evolution of normal intestinal mucosa-intestinal adenoma-intestinal cancer axis and explored that *Fusobacteria* might be a novel biomarker for the identification of CRA and CRC.

7. Funding

This work was supported by the National Key R&D Program of China (2018YFC1313300), the National Natural Science Foundation of China (No.81472707) and Chinese South Western Oncology Group (CSWOG-CCET005).

References

1. Siegel RL, Miller KD, Fedewa SA, Ahnen DJ, Meester RGS, Barzi A, et al. Colorectal cancer statistics, 2017. *CA Cancer J Clin.* 2017; 67: 177-93.
2. Chen W, Zheng R, Baade PD, Zhang S, Zeng H, Bray F, et al. Cancer statistics in China, 2015. *CA Cancer J Clin.* 2016; 66: 115-32.
3. Markowitz SD, Bertagnolli MM. Molecular origins of cancer: Molecular basis of colorectal cancer. *N Engl J Med.* 2009; 361: 2449-60.
4. Song M, Chan AT. Environmental Factors, Gut Microbiota, and Colorectal Cancer Prevention. *Clin Gastroenterol Hepatol.* 2019; 17: 275-89.

5. Bultman SJ. Molecular pathways: gene-environment interactions regulating dietary fiber induction of proliferation and apoptosis via butyrate for cancer prevention. *Clin Cancer Res.* 2014; 20: 799-803.
6. Song M, Garrett WS, Chan AT. Nutrients, foods, and colorectal cancer prevention. *Gastroenterology.* 2015; 148: 1244-60 e16.
7. Yang Y, Misra BB, Liang L, Bi D, Weng W, Wu W, et al. Integrated microbiome and metabolome analysis reveals a novel interplay between commensal bacteria and metabolites in colorectal cancer. *Theranostics.* 2019; 9: 4101-14.
8. O'Keefe SJ. Diet, microorganisms and their metabolites, and colon cancer. *Nat Rev Gastroenterol Hepatol.* 2016; 13: 691-706.
9. He J, Li Y, Cao Y, Xue J, Zhou X. The oral microbiome diversity and its relation to human diseases. *Folia Microbiol (Praha).* 2015; 60: 69-80.
10. de Martel C, Ferlay J, Franceschi S, Vignat J, Bray F, Forman D, et al. Global burden of cancers attributable to infections in 2008: a review and synthetic analysis. *Lancet Oncol.* 2012; 13: 607-15.
11. Schwabe RF, Jobin C. The microbiome and cancer. *Nat Rev Cancer.* 2013; 13: 800-12.
12. Yu J, Feng Q, Wong SH, Zhang D, Liang QY, Qin Y, et al. Metagenomic analysis of faecal microbiome as a tool towards targeted non-invasive biomarkers for colorectal cancer. *Gut.* 2017; 66: 70-8.
13. Flemer B, Lynch DB, Brown JM, Jeffery IB, Ryan FJ, Claesson MJ, et al. Tumour-associated and non-tumour-associated microbiota in colorectal cancer. *Gut.* 2017; 66: 633-43.
14. Feng Q, Liang S, Jia H, Stadlmayr A, Tang L, Lan Z, et al. Gut microbiome development along the colorectal adenoma-carcinoma sequence. *Nat Commun.* 2015; 6: 6528.
15. Peters BA, Wu J, Pei Z, Yang L, Purdue MP, Freedman ND, et al. Oral Microbiome Composition Reflects Prospective Risk for Esophageal Cancers. *Cancer Res.* 2017; 77: 6777-87.
16. Park CH. Early diagnosis of hepatocellular carcinoma using imaging modalities. *Yonsei Med J.* 1988; 29: 101-8.
17. Koliarakis I, Messaritakis I, Nikolouzakis TK, Hamilos G, Souglakos J, Tsiaoussis J. Oral Bacteria and Intestinal Dysbiosis in Colorectal Cancer. *Int J Mol Sci.* 2019; 20.
18. smoking and colorectal cancer. *J Epidemiol Res.* 2016; 2: 92-101.
19. Yang Y, Cai Q, Shu XO, Steinwandel MD, Blot WJ, Zheng W, et al. Prospective study of oral microbiome and colorectal cancer risk in low-income and African American populations. *Int J Cancer.* 2019; 144: 2381-9.
20. Brennan CA, Garrett WS. Gut Microbiota, Inflammation, and Colorectal Cancer. *Annu Rev Microbiol.* 2016; 70: 395-411.
21. Mima K, Sukawa Y, Nishihara R, Qian ZR, Yamauchi M, Inamura K, et al. *Fusobacterium nucleatum* and T Cells in Colorectal Carcinoma. *JAMA Oncol.* 2015; 1: 653-61.
22. Flanagan L, Schmid J, Ebert M, Soucek P, Kunicka T, Liska V, et al. *Fusobacterium nucleatum* associates with stages of colorectal neoplasia development, colorectal cancer and disease outcome. *Eur J Clin Microbiol Infect Dis.* 2014; 33: 1381-90.
23. Castellarin M, Warren RL, Freeman JD, Dreolini L, Krzywinski M, Strauss J, et al. *Fusobacterium nucleatum* infection is prevalent in human colorectal carcinoma. *Genome Res.* 2012; 22: 299-306.
24. Bray C, Bell LN, Liang H, Collins D, Yale SH. Colorectal Cancer Screening. *WMJ.* 2017; 116: 27-33.
25. Sung JJ, Ng SC, Chan FK, Chiu HM, Kim HS, Matsuda T, et al. An updated Asia Pacific Consensus Recommendations on colorectal cancer screening. *Gut.* 2015; 64: 121-32.
26. Nieuwdorp M, Gilijamse PW, Pai N, Kaplan LM. Role of the microbiome in energy regulation and metabolism. *Gastroenterology.* 2014; 146: 1525-33.
27. Devaraj S, Hemarajata P, Versalovic J. The human gut microbiome and body metabolism: implications for obesity and diabetes. *Clin Chem.* 2013; 59: 617-28.
28. Cani PD. Gut cell metabolism shapes the microbiome. *Science.* 2017; 357: 548-9.
29. Wixon J, Kell D. The Kyoto encyclopedia of genes and genomes--KEGG. *Yeast.* 2000; 17: 48-55.
30. Ito M, Kanno S, Nosho K, Sukawa Y, Mitsuhashi K, Kurihara H, et al. Association of *Fusobacterium nucleatum* with clinical and molecular features in colorectal serrated pathway. *Int J Cancer.* 2015; 137: 1258-68.
31. Kostic AD, Gevers D, Pedamallu CS, Michaud M, Duke F, Earl AM, et al. Genomic analysis identifies association of *Fusobacterium* with colorectal carcinoma. *Genome Res.* 2012; 22: 292-8.
32. Kostic AD, Chun E, Robertson L, Glickman JN, Gallini CA, Michaud M, et al. *Fusobacterium nucleatum* potentiates intestinal tumorigenesis and modulates the tumor-immune microenvironment. *Cell Host Microbe.* 2013; 14: 207-15.
33. Rubinstein MR, Wang X, Liu W, Hao Y, Cai G, Han YW. *Fusobacterium nucleatum* promotes colorectal carcinogenesis by modulating E-cadherin/beta-catenin signaling via its FadA adhesin. *Cell Host Microbe.* 2013; 14: 195-206.
34. Gagniere J, Raisch J, Veziat J, Barnich N, Bonnet R, Buc E, et al. Gut microbiota imbalance and colorectal cancer. *World J Gastroenterol.* 2016; 22: 501-18.
35. Nakatsu G, Li X, Zhou H, Sheng J, Wong SH, Wu WK, et al. Gut mucosal microbiome across stages of colorectal carcinogenesis. *Nat Commun.* 2015; 6: 8727.
36. Kumarakulasingham M, Rooney PH, Dundas SR, Telfer C, Melvin WT, Curran S, et al. Cytochrome p450 profile of colorectal cancer: identification of markers of prognosis. *Clin Cancer Res.* 2005; 11: 3758-65.
37. Lanzetti L, Di Fiore PP. Endocytosis and cancer: an 'insider' network with dangerous liaisons. *Traffic.* 2008; 9: 2011-21.